HAL open science

Influence of Anisotropy on Fluid-Structure Interaction Simulations of Image-Based and Generic Mitral Valves

Nariman Khaledian, Pierre-Frédéric Villard, Peter E. Hammer, Douglas P. Perrin, Marie-Odile Berger

▶ **To cite this version:**

Nariman Khaledian, Pierre-Frédéric Villard, Peter E. Hammer, Douglas P. Perrin, Marie-Odile Berger. Influence of Anisotropy on Fluid-Structure Interaction Simulations of Image-Based and Generic Mitral Valves. The 12th International Conference On Functional Imaging And Modeling Of The Heart, Jun 2023, Lyon, France. pp.455-464, 10.1007/978-3-031-35302-4_47 . hal-04117508

HAL Id: hal-04117508

https://hal.science/hal-04117508

Submitted on 5 Jun 2023

HAL is a multi-disciplinary open access archive for the deposit and dissemination of scientific research documents, whether they are published or not. The documents may come from teaching and research institutions in France or abroad, or from public or private research centers.

L'archive ouverte pluridisciplinaire **HAL**, est destinée au dépôt et à la diffusion de documents scientifiques de niveau recherche, publiés ou non, émanant des établissements d'enseignement et de recherche français ou étrangers, des laboratoires publics ou privés.

Distributed under a Creative Commons Attribution 4.0 International License

Influence of Anisotropy on Fluid-Structure Interaction Simulations of Image-Based and Generic Mitral Valves

Nariman Khaledian[1], Pierre-FrédéricVillard[1,3], Peter E. Hammer[2], Douglas P. Perrin[2,3], and Marie-Odile Berger[1]

[1] Université de Lorraine, CNRS, Inria, LORIA, Nancy, France
[2] Harvard Medical School, Boston, MA, USA
[3] Harvard School of Engineering and Applied Sciences, Cambridge, MA, USA

Abstract. The dynamic behavior of the mitral valve is highly influenced by the material model used to describe the leaflet motion. Due to the presence of collagen fibers, mitral valve leaflets show an anisotropic behavior. The aim of this study is to investigate the influence of anisotropy on fluid-structure simulations of the mitral valve dynamic closure. The fluid-structure simulation of the mitral valve is performed using an immersed boundary method. Two constitutive models, Holzapfel-Gasser-Ogden for the anisotropic, and third-order Ogden for the isotropic are used. For the anisotropic model, two fiber directions, one that is parallel to the annulus surface and another that follows an arc on the leaflets are considered. In order to take into account the effects of both the chordae structure and leaflet geometry, generic and image-based mitral valves are studied. The quality of the closure is evaluated based on measuring the bulging area, contact map, and flow rate. In both generic and image-based, a significant difference is observed between the anisotropic and isotropic cases. Additionally, The chordae forces during the closure are compared with ex-vivo data of the literature. The results indicate that the anisotropic model with arc-based fibers exhibits a similar pattern.

Keywords: Mitral valve · Fluid-structure interaction · anisotropy.

1 Introduction

The mitral valve (MV) ensures the one-way flow of oxygenated blood from the left atrium to the left ventricle. It consists of leaflets that are held in a closed position by chordae. Various pathologies reduce its efficiency of remaining sealed properly and surgery may be necessary to repair the valve. Unfortunately, it depends on the surgeon's experience as well as on the patient's data. Computer-based simulations can help to have a predictive treatment.

In [13], a Fluid-Structure Interaction (FSI) method has been studied to simulate the MV behavior by focusing on perfect closure with no orifice hole. A generic MV geometry and isotropic hyperelastic material model were used. It was shown that it is possible to have a reliable simulation that can predict if a

valve is pathological in a reasonable time. However, the chordae structure, the leaflet geometry, and the microstructure of the leaflet tissue are unique for each patient. We propose here to go toward clinical use and then replicate the accurate behavior of the MV. Two steps are necessary: extracting the image-based patient's valve anatomy and simulating the valve closure with real biomechanical parameters and real boundary conditions.

In this paper, we focus on those two aspects. The image-based geometry is extracted from the segmentation of a medical image and it leads to various challenges compared to generic geometry. The leaflets have non-regular contours with some noise. Many folds can occur during the closing process. Real chordae have a less homogeneous architecture and some parts could be missed easily by the segmentation. We study the impact of such a geometry. The real mechanical behavior of the valve includes replicating the tissue microstructure that is known to be anisotropic. We study the influence of the anisotropy both on a generic and an image-based valve as well as its influence on the valve shape.

2 State of the art

Various experimental studies like [14] measured the stress-strain response of MV leaflet. It is observed that the leaflet tissue shows anisotropic behavior and that anisotropy rates depend on the region where the specimen is taken for the stress-strain test. This can be explained by considering leaflet tissue as a composite of fiber families running through an isotropic base material and assuming that fiber orientation dictates the anisotropy rate. The fiber map can be extracted by using small angle light scattering (SALS) to observe the micro-structure of the leaflet [23]. The fiber map is unique for each specimen and obtaining it is a time-consuming work and needs resources and expertise in conducting experimental studies. To have a practical simulation, that can be used for any patient-specific case, simplification in modeling different aspects of the MV is inevitable. In the literature, fibers are modeled by implementing the fiber map extracted from observing the micro-structure of the leaflets as described in [23, 25, 3, 16], or simply laying the fibers to be parallel to the annulus as described in [12, 27, 29]. One attempt to come up with a global fiber map is done by Einstein et al [7], they used the SALS data reported in [5]. This fiber map is used in [6, 21, 26] and it follows two rules, in the middle of the leaflet being parallel to the annulus, and close to the commissures being perpendicular to the free edge. The influence of fiber direction in the simulation results is described in [12].

In the literature, various constitutive models are used to model the anisotropic behavior of the MV leaflets. These models can be categorized as coupled [17] and decoupled [10]. May-Newman et al [17] proposed an anisotropic constitutive model specific for MV leaflets in which the strain energy function consists of a single term describing the material behavior in all directions. In decoupled models, such as Holzapfel-Gasser-Ogden (HGO) constitutive model [10], the strain energy function consists of one isotropic and one anisotropic term which in combination describes the desired anisotropic behavior. In [23] performance of both

coupled and decoupled anisotropic models is compared to in vivo measurement on ovine data with shell structure simulations.

Extracting the coefficients of these models can be challenging. Extracting the 3D coefficients of a generalized Fung model is impossible since it requires shear data in all three main directions, whereas only planar biaxial tests are possible. In [2], an inverse finite element study is used to optimize the constitutive model coefficients based on in vitro experimental study. In the case of HGO model, the strain energy function consists of one linear and one exponential term with four different coefficients. This will make it more challenging to fit experimental data and the success of the optimization relies on the initial values of the coefficients.

Depending on the purpose of the study, the geometry used in the literature is generic valve [12], parameterized valve [21], or image-based In that case, the objective is to work with realistic geometry and to address patient-specific data or pathologies. Since the complete chordae network is not visible under clinical imaging modalities, many works use generic evenly distributed chordae tendineae [9], adapt existing data to a specific patient[1], or use ex-vivo setup to obtain clean and high-resolution subject-specific mitral valve imaging [28]. Most of the time, the annulus is approximated with a circular or elliptic shape, or cubic Hermitian splines [23] though its real shape is much more complex [19].Only a small number of papers address MV simulation with image-based leaflet and chordae geometry as [8] who investigate how chordae structure impacts the MV dynamics and [24] in the context of prolapsus study. Globally, the aim of these studies is to perform comparisons between different configurations but the effectiveness of closure is not the central topic of these studies though it is a fundamental clinical topic.

Our contributions are twofold: define a FSI model able to handle image-based data and experimental-based tissue properties, and study the added value of this improved model on porcine data. More specifically:

- we first explicitly describe in section 3 the changes in the FSI model which are required to handle real valve obtained from image segmentation and specifically: complex and irregular leaflet surfaces, non-elliptic annulus shapes, trees of chordae.
- we study the impact of using isotropic versus anisotropic material on the realism of the simulation. Our study is based on the HGO model which is one of the most widely used anisotropic hyperelastic models. We then study how fiber direction influences the simulation.
- The efficiency of the models are measured with several figures of merits that allow us to evaluate the valve closure: bulging ratio, map of contact, forces applied on the chordae and flow rate.

3 Method

The method for simulating MV closure is based on the FSI immersed boundary method described in [13] and demonstrated for a generic valve. We describe in

the section the changes which were necessary to adapt this model to image-based data.

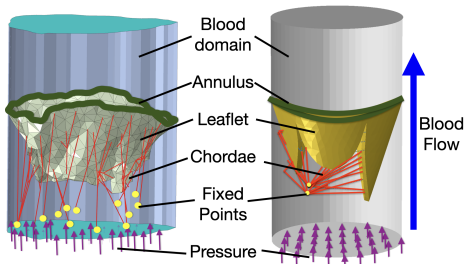

Fig. 1. Case set-up showing the image-based (left) and generic (right) MV mounted in an a generalized and a elliptic cylinder.

Geometry: Two kinds of MV geometry have been studied. A generic one like in [13] and a image-based one extracted from a 3D CT scan of an explanted porcine heart. In the generic geometry case, the chordae structure is optimal such as the valve always closes. In the case of the geometry extracted from medical data, the leaflets and the chordae have been manually segmented at the open state of the valve. This porcine valve closes naturally ex-vivo without orifice holes. The chordae structure is represented by a linear elastic two-nodes beam element with an articulated mechanism to avoid compression load in the chordae. MV is immersed in a tube filled with blood representing the fluid domain. The tube in the generic valve is relatively simple with an elliptic base, but the image-based valve has a more complex annulus shape. The tube base is the shape of the annulus ring to prevent blood pass over the annulus. The tube direction is normal to the annulus plane and is determined thanks to a principal component analysis on the vertices of the annulus ring (see Fig.1). The numerical domain in the image-based valve has $28k$ elements for the leaflets and $34k$ elements for the blood. In the case of the generic valve, the leaflets are represented with $40k$ elements, and the blood consists of $65k$ elements.

Numerical domain: The tube is represented by a C3D8 element, a hexahedron with one node in each corner, with reduced integration. For the more complex geometry of the image-based valve, the C3D4 element, a tetrahedron with one node in each corner, is used which has better convergence qualities compared to the C3D10 element, a tetrahedron with one node in each corner and an extra node in the middle of each edge, previously used for generic valve with less complex geometry in [13]. The quadratic nature of C3D10 is not suitable when element nodes on complex surfaces are included in a contact model. Therefore, C3D4 is relatively less prone to distortion in such situations and prevents divergence of the simulation caused by element distortion.

In image-based MV geometry, the angle between the leaflet facets is relatively sharper compared to the generic valve. This makes contact behavior more com-

plex by assuming that neighboring facets are constantly going to be engaged in contact. The simulation with the image-based valve diverges when both sides of the leaflet with 1mm thickness are involved in the contact model. Therefore, only the inner surface of the leaflets is included in the contact model. The self-contact between the leaflet surfaces is modeled by using the balanced master-slave technique. The normal forces are computed with a penalty-based formulation, and frictional contact is calculated by Coulomb's friction model [13].

Constitutive model: To mimic the anisotropic behavior of the MV leaflets, we used the HGO constitutive model [10] which is already used in the literature for modeling the biological tissues. The HGO strain energy function for the incompressible material is as follows:

$$\psi = C_{10}(I_1 - 3) + K_1/2K_2 \sum_{\alpha=1}^{N}[exp(K_2 < E_\alpha >^2) - 1] \tag{1}$$

In this model, the anisotropic behavior is introduced by families of fibers running through a uniform medium. The C_{10} coefficient in the linear part of the equation defines the characteristics of the uniform medium. K_1 and K_2 define the behavior of tension-only fibers. One family of fibers, $N = 1$, is defined in the simulation. $E_\alpha = \kappa(I_1-3)+(1-3\kappa)(I_{4(\alpha\alpha)}-1)$ which I_1 is the first deviatoric strain invariant, $I_{4(\alpha\alpha)}$ is the pseudo-invariant related to the fibers, and κ is the dispersion factor between zero, parallel fiber families, to 1/3, randomly distributed fibers.

The direction of fibers is an important factor influencing the mechanical response of the MV. Experimental studies, for example in [5], confirm that in the central region of the leaflets, fibers are parallel to the annulus. The fiber direction in other regions of the leaflet is specific for each valve, but the general trend is that in the anterior and posterior leaflets, fibers follow an arc from one side of the leaflet to another [18, 22], joining one group of chordae endpoints to another. To evaluate the performance of this fiber direction, we consider in this study two fiber directions. One parallel to the annulus surface, and one following an arc by using diffusion to determine the fiber direction in each element (Fig. 2).

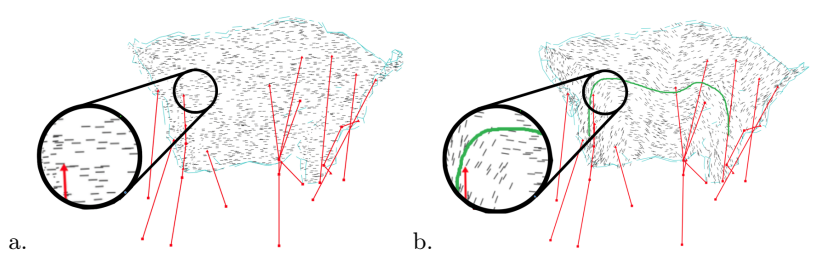

Fig. 2. Fiber map on the anterior leaflet of the image-based valve: (a) with parallel-based fibers (b) with the curve-based approach after the diffusion process.

Calibration of Material parameters: HGO coefficients (C_{10}, K_1, K_2) for porcine MV are not reported in the literature. Indeed, Such parameters are avail-

able for ovine data in [23] or for porcine data but only for the aortic valve [15]. Therefore, we decided to use stress-strain experimental data from [11] to extract the proper coefficients for our simulation. The optimization process is done with the MCalibration software[4] which is connected to Abaqus solver to execute the inverse finite element analysis calculations. Depending on the chosen optimization technique, the results turn out to be unstable and sensitive to the initial estimate. We thus use genetic algorithms for minimization and consider several plausible initial values and keep the one that provides the smallest residual.

The parameters computed with this method are the following: $C_{10} = 2272$, $K_1 = 4000, K_2 = 150$, $\kappa = 0.25$. To obtain the isotropic material parameters comparable with the anisotropic one, first, the dispersion coefficient, κ, is set to the maximum, 1/3, which makes the constitutive model act as isotropic. The stress-strain response is then extracted and used as material behavior to obtain the third-order Ogden hyperelastic constitutive model, which results in the following final coefficients for the isotropic mode: $\mu_1 = -481836.3$, $\alpha_1 = -19.4$, $\mu_2 = 484166.6$, $\alpha_2 = -19.3$, $\mu_3 = 742.8$, $\alpha_3 = -25$.

4 Results and discussion

We compare in this section the simulations obtained with and without considering anisotropy in the case of a generic and a real valve, with the same HGO parameters. Results are provided in Fig. 3 top row for the generic valve and in Fig. 3 bottom row, 4, and 5 for the image-based valve. Two fibers models are considered in the anisotropic case (Fig. 2): parallel to the annulus (denoted as anisotropic with parallel-based fibers) and fibers guided by diffusion following one arc outlined by an expert (denoted as anisotropic with arc-based fibers). Both for generic and image-based cases, the use of isotropic model induces a high bulging of the leaflet (see Fig. 3 top and bottom rows where parts above the annular plane are drawn in red), whereas anisotropy shows a decreased bulging. This fact is in good agreement with clinical knowledge which states that "A normal mitral valve has [...] a large surface of coaptation with the free edge positioned low below the plane of the orifice" [4]. The other interesting fact is that we are able to replicate the imbalanced chordae forces between primary and secondary chordae which were measured ex vivo in [20] and are reproduced in Fig. 4.a. Our simulations during closure have to be compared to this graph in the time interval $[0.1 - 0.2]$ seconds. As can be seen on Fig.4.b, the simulation with isotropy fails to reproduce the primary and secondary chords behavior. On the contrary, the simulations with anisotropy are closer to the reference, and isotropic with arc-based fibers faithfully reproduces the order of magnitude of forces.

The map of contact forces obtained with the anisotropic model are presented in Fig. 5 for isotropic (a), anisotropic with parallel-based fibers (b), and anisotropic with arc-based fibers (c). The cumulative map, i.e. $P(||pressure|| >$

[4] https://polymerfem.com/mcalibration/

t) is also provided (Fig. 5.d). The map is very irregular and not realistic in the isotropic case because the high bulging produces folds with high contacts near the annulus. With fibers parallel to the annulus, the area of contacts is roughly parallel to the annulus and shows areas with higher contact forces. When curve-based fibers are used, the amplitude of contacts is higher than with the two other cases as can be seen on the cumulative map. The flow rates are shown for each case in Fig. 4.e and show that the mitral valve closure is effective for the three cases. These experiments confirm that arc-based fibers allow a more realistic simulation than the other models. Indeed the valve we model is structurally normal and such valves do not exhibit significant bulging above the annulus. The model anisotropic with arc-based fibers best reproduces this expected behavior. This model also produces a force map which faithfully mimics ex-vivo data available in the literature. Finally, it also produces the strongest contact force.

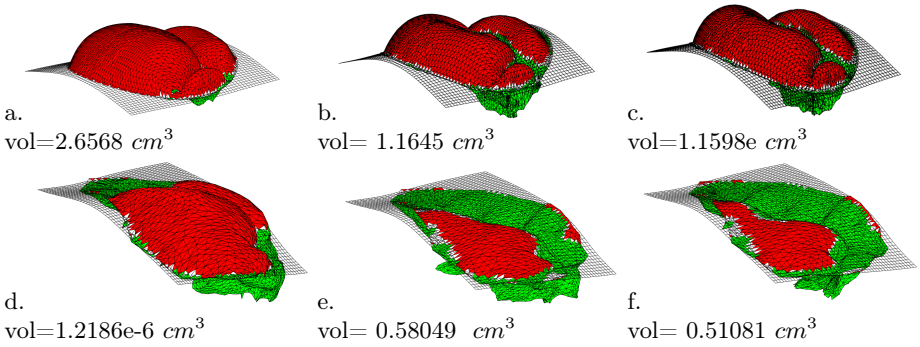

Fig. 3. Top row: bulging on the generic valve with (a) isotropic, (b)anisotropic with parallel-based fibers, (c) anisotropic with arc-based fibers. Bottom row: bulging on the image-based valve with (d) isotropic, (e) anisotropic with parallel-based fibers, (f) anisotropic with arc-based fibers.

5 Conclusion

In this paper, we studied the influence of an anisotropy constitutive law on the MV using FSI analysis. The impact of the anisotropy has first been shown on a generic geometry where closure is ensured by an optimum chordae architecture. Less bulging was noticed with anisotropy compared to isotropy. Then, an imaged-based valve was used with manually segmented chordae and leaflets leading to a more irregular geometry. We tested the influence of isotropy and anisotropy with two fiber directions dictated by rules from the literature. Once again, less bulging is observed with anisotropy and a more detailed analysis also showed more cues that correctly match with clinical observations.

In future work, we planned to focus on a new strategy to extract a more complex fiber map based on the chordae structure. The chordae are known to

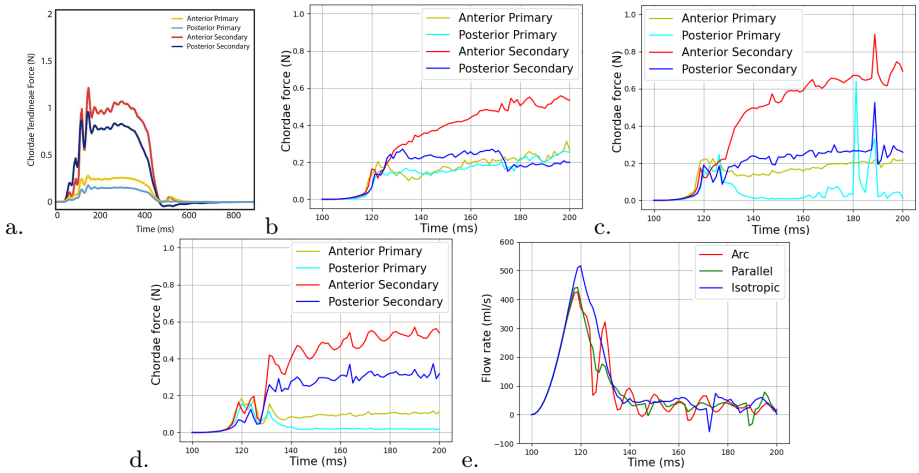

Fig. 4. Chordae force distribution on ex-vivo data from [20] (a), simulation with isotropic (b), anisotropic with parallel-based fibers (c), anisotropic with arc-based fibers (d), Flow rates through time (e).

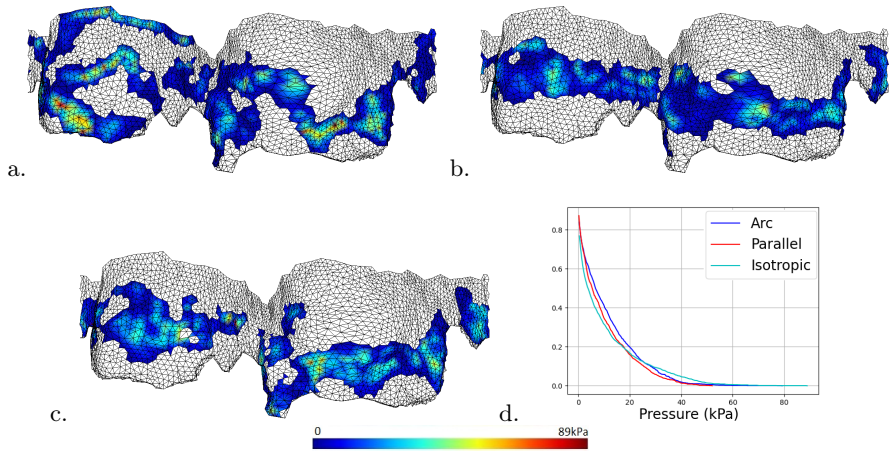

Fig. 5. Contact map with isotropic (a), anisotropic with parallel-based fibers (b), anisotropic with arc-based fibers (c), cumulative distribution (d)

be dense bundles of parallel, load-bearing fibers, and we can assume that these fibers are in continuity with the leaflets in the regions at which they insert.

References

1. A workflow for patient-specific fluid-structure interaction analysis of the mitral valve: A proof of concept on a mitral regurgitation case. Medical Engineering & Physics **74**, 153–161 (2019)
2. Abbasi, M., Barakat, M.S., Vahidkhah, K., Azadani, A.N.: Characterization of three-dimensional anisotropic heart valve tissue mechanical properties using inverse finite element analysis. Journal of the mechanical behavior of biomedical materials **62**, 33–44 (2016)
3. Amini, R., Eckert, C.E., Koomalsingh, K., McGarvey, J., Minakawa, M., Gorman, J.H., Gorman, R.C., Sacks, M.S.: On the in vivo deformation of the mitral valve anterior leaflet: effects of annular geometry and referential configuration. Annals of biomedical engineering **40**(7), 1455–1467 (2012)
4. Carpentier, A., Adams, D.H., Filsoufi, F.: Carpentier's reconstructive valve surgery : from valve analysis to valve reconstruction. Elsevier (2010)
5. Cochran, R., Kunzelman, K., Chuong, C., Sacks, M., Eberhart, R.: Nondestructive analysis of mitral valve collagen fiber orientation. ASAIO transactions **37**(3), M447–8 (1991)
6. Einstein, D.R., Kunzelman, K., Reinhall, P., Nicosia, M., Cochran, R.: Haemodynamic determinants of the mitral valve closure sound: a finite element study. Medical and Biological Engineering and Computing **42**(6), 832–846 (2004)
7. Einstein, D.R., Kunzelman, K.S., Reinhall, P.G., Nicosia, M.A., Cochran, R.P.: The relationship of normal and abnormal microstructural proliferation to the mitral valve closure sound. J. Biomech. Eng. **127**(1), 134–147 (2005)
8. Feng, L., Qi, N., Gao, H., Sun, W., Vazquez, M., Griffith, B., Luo, X.: On the chordae structure and dynamic behaviour of the mitral valve. IMA J Appl Math. **83**(6), 1066–1091 (2018)
9. Gao, H., Feng, L., Qi, N., Berry, C., Griffith, B.E., Luo, X.: A coupled mitral valve—left ventricle model with fluid–structure interaction. Medical Engineering & Physics **47**, 128–136 (2017)
10. Gasser, T.C., Ogden, R.W., Holzapfel, G.A.: Hyperelastic modelling of arterial layers with distributed collagen fibre orientations. Journal of the royal society interface **3**(6), 15–35 (2006)
11. Jett, S., Laurence, D., Kunkel, R., Babu, A.R., Kramer, K., Baumwart, R., Towner, R., Wu, Y., Lee, C.H.: An investigation of the anisotropic mechanical properties and anatomical structure of porcine atrioventricular heart valves. Journal of the mechanical behavior of biomedical materials **87**, 155–171 (2018)
12. Kaiser, A.D., McQueen, D.M., Peskin, C.S.: Modeling the mitral valve. International Journal for Numerical Methods in Biomedical Engineering **35**(11) (2019)
13. Khaledian, N., Villard, P.F., Berger, M.O.: Capturing contact in mitral valve dynamic closure with fluid-structure interaction simulation. International Journal of Computer Assisted Radiology and Surgery pp. 1–8 (2022)
14. Laurence, D., Ross, C., Jett, S., Johns, C., Echols, A., Baumwart, R., Towner, R., Liao, J., Bajona, P., Wu, Y., et al.: An investigation of regional variations in the biaxial mechanical properties and stress relaxation behaviors of porcine atrioventricular heart valve leaflets. Journal of biomechanics **83**, 16–27 (2019)

15. Laville, C., Pradille, C., Tillier, Y.: Mechanical characterization and identification of material parameters of porcine aortic valve leaflets. Journal of the mechanical behavior of biomedical materials **112**, 104036 (2020)
16. Lee, C.H., Amini, R., Gorman, R.C., Gorman III, J.H., Sacks, M.S.: An inverse modeling approach for stress estimation in mitral valve anterior leaflet valvuloplasty for in-vivo valvular biomaterial assessment. Journal of biomechanics **47**(9), 2055–2063 (2014)
17. May-Newman, K., Yin, F.C.P.: A Constitutive Law for Mitral Valve Tissue. Journal of Biomechanical Engineering **120**(1), 38–47 (1998)
18. Noack, T., Kiefer, P., Ionasec, R., Voigt, I., Mansi, T., Vollroth, M., Hoebartner, M., Misfeld, M., Mohr, F.W., Seeburger, J.: New concepts for mitral valve imaging. Annals of cardiothoracic surgery **2**(6), 787 (2013)
19. Panicheva, D., Villard, P.F., Hammer, P.E., Perrin, D., Berger, M.O.: Automatic extraction of the mitral valve chordae geometry for biomechanical simulation. International Journal of Computer Assisted Radiology and Surgery pp. 709–720 (2021)
20. Paulsen, M.J., Bae, J.H., Imbrie-Moore, A.M., Wang, H., Hironaka, C.E., Farry, J.M., Lucian, H., Thakore, A.D., Cutkosky, M.R., Joseph Woo, Y.: Development and Ex Vivo Validation of Novel Force-Sensing Neochordae for Measuring Chordae Tendineae Tension in the Mitral Valve Apparatus Using Optical Fibers With Embedded Bragg Gratings. Journal of Biomechanical Engineering **142**(1) (10 2019)
21. Prot, V., Haaverstad, R., Skallerud, B.: Finite element analysis of the mitral apparatus: annulus shape effect and chordal force distribution. Biomechanics and modeling in mechanobiology **8**(1), 43–55 (2009)
22. Prot, V., Skallerud, B.: Nonlinear solid finite element analysis of mitral valves with heterogeneous leaflet layers. Computational Mechanics **43**(3), 353–368 (2009)
23. Rausch, M.K., Famaey, N., Shultz, T.O., Bothe, W., Miller, D.C., Kuhl, E.: Mechanics of the mitral valve. Biomechanics and modeling in mechanobiology **12**(5), 1053–1071 (2013)
24. Razavi, S.E., Talebi, A.: Comparative modeling of the mitral valve in normal and prolapse conditions. Bioimpacts (2023)
25. Sadeghinia, M.J., Skallerud, B., Holzapfel, G.A., Prot, V.: Biomechanics of mitral valve leaflets: Second harmonic generation microscopy, biaxial mechanical tests and tissue modeling. Acta biomaterialia **141**, 244–254 (2022)
26. Skallerud, B., Prot, V., Nordrum, I.: Modeling active muscle contraction in mitral valve leaflets during systole: a first approach. Biomechanics and modeling in mechanobiology **10**(1), 11–26 (2011)
27. Stevanella, M., Votta, E., Redaelli, A.: Mitral valve finite element modeling: implications of tissues' nonlinear response and annular motion. Journal of biomechanical engineering **131**(12) (2009)
28. Toma, M., Bloodworth, C., Einstein, D., Pierce, E., Cochran, R., Yoganathan, A., Kunzelman, K.: High resolution subject-specific mitral valve imaging and modeling: Experimental and computational methods. Biomechanics and Modeling in Mechanobiology **15** (12 2016). https://doi.org/10.1007/s10237-016-0786-1
29. Votta, E., Caiani, E., Veronesi, F., Soncini, M., Montevecchi, F.M., Redaelli, A.: Mitral valve finite-element modelling from ultrasound data: a pilot study for a new approach to understand mitral function and clinical scenarios. Philosophical Transactions of the Royal Society A: Mathematical, Physical and Engineering Sciences **366**(1879), 3411–3434 (2008)